

Temperature Control of a Target Plate under Variable Flow of Impinging Air from an Orifice

Dr. Adnan A. Abdel Rasool

Engineering College, University of Al-Mustansiriya /Baghdad

Email: adn1954@yahoo.com

Dr. Yahya A. Faraj

Engineering College, University of Al-Mustansiriya /Baghdad

Email: Aliyahya@yahoo.com

Roaad K. Mohammed A.

Engineering College, University of Al-Mustansiriya /Baghdad

Email: roody_eng@yahoo.com

Received on:19/3/2014 & Accepted on :6/11/2014

ABSTRACT

This work concerns with experimental and numerical study for the cooling characteristics of a target plate under the effect of air impingement from orifice of different sizes D of (5,10,15 and 20 mm). A centrifugal blower was used for air impinging with jet velocity in the range (18-40 m/s). Tested Reynolds number Re is in the range of (7100-44400) with orifice to plate spacing ratio H/D of (2,4,6,8). Numerical analysis using CFD commercial code Fluent version 14.5 with $K-\epsilon$ RNG turbulence model has been used to simulate the flow and heat transfer in impingement jet. Both numerical and experimental results are analyzed to determine the effect of using different orifice sizes on heat transfer rates and flow structure on the target plate. A correlation is obtained for the stagnation Nusselt number as a function of Re and H/D . Optimum heat removal rate are found to occur at $H/D=6$. According to the experimental results which indicates that orifice diameter and jet velocity are the most effective variables which characterize the heat removal rate, a control system is designed and constructed to vary the orifice diameter in order to control the air flow rate and the plate temperature. Fixing the optimum H/D and for the used blower characteristics the control system is tested and the results show a good response for the control system for different operation conditions so that the cooling rates are increased for the heated plate.

Keywords: Impingement Jet, Flat Plate, Cooling, Numerical Simulation, Temperature Control.

السيطرة على درجة حرارة صفيحة معرضة لنفث هواء تصادمي متغير من فوهة

الخلاصة

يتناول البحث دراسة عملية و عددية لخصائص التبريد لصفيحة معرضة لتبريد تصادمي من فوهة ذات قطر (5, 10, 15, و 20 ملم). تم استخدام منفاخ طارد مركزي ليثق الهواء بمعدل سرعة (18-40 م/ث). رقم رينولدز في حدود (44400-7100) و نسبة بعد الصفيحة الهدف عن الفوهة الى القطر (2, 4, 6, 8). وقد استخدم التحليل العددي بطريقة CFD البرنامج Fluent الاصدار 14.5 مع موديل الجريان الاضطرابي K-ε RNG نموذجاً لمحاكاة تدفق وانتقال الحرارة في التبريد التصادمي. تم تحليل النتائج العملية و النظرية لإيجاد تأثير قطر الفوهة على انتقال الحرارة و طبيعة الجريان على الصفيحة الهدف. تم الحصول على معادلة لعدد نسلت في منطقة الركود بالاعتماد على عدد رينولدز و نسبة بعد الصفيحة عن الفوهة الى القطر. لوحظ ان افضل معدل لإزالة الحرارة يحدث عند $H/D=6$. وفقاً للنتائج التجريبية التي تشير إلى أن قطر الفتحة و سرعة الهواء هما المتغيران الأكثر فعالية التي تميز معدل إزالة الحرارة. تم تصميم منظومة تحكم لتغيير قطر الفوهة من أجل التحكم في معدل تدفق الهواء ودرجة حرارة الصفيحة الهدف. تم اختبار منظومة التحكم بالاعتماد على H/D الأمثل و خصائص المنفاخ المستخدم و اظهرت النتائج استجابة جيدة عند ظروف تشغيل مختلفة بحيث زادت معدلات التبريد في الصفيحة المسخنة .

NOMENCLATURE

| | |
|---------------|--|
| D | Orifice diameter (m) |
| H/D | Target plate to nozzle diameter spacing ratio (dimensionless) |
| h | Heat transfer coefficient ($W/m^2 \cdot ^\circ C$) |
| K_j | Conductivity of air at film temperature ($W/m \cdot ^\circ C$) |
| K | Conductivity of stainless steel plate ($W/m \cdot ^\circ C$) |
| Nu | Nusselt number (dimensionless) = $\frac{hD}{K}$ |
| $q''_{conv.}$ | Heat flux by convection (W/m^2) |
| Re | Reynolds number (dimensionless) = $\frac{U_j D}{\nu_j}$ |
| R | Orifice radius (m) |
| r | Radial distance from the plate center (m) |
| S.P | Set Point |
| T_f | Film temperature ($^\circ C$) = $\frac{T_s + T_j}{2}$ |
| T_s | The temperature at the surface of the plate ($^\circ C$) |
| T_j | The jet-stream temperature ($^\circ C$) |
| t | Thickness of stainless steel plate (m) |
| U_j | Velocity of air (m/s) |
| δ | Boundary layer thickness (mm) |
| ϕ | Dependent variable |
| Γ_ϕ | Diffusion coefficient |
| k-ε | Two-equations turbulence model |
| μ_{eff} | Effective viscosity ($N \cdot s/m^2$) |
| ν_j | Kinematic viscosity of air at film temperature (m^2/s) |
| S_ϕ | Source term |

INTRODUCTION

Impinging jets is widely used in different industrial applications due to high rate of heat removal on the surface being subjected to impinging. Such technique is used in cooling, heating and drying of papers or textiles, processing of steel or glass, electrical equipment coolingetc.

A lot of numerical and experimental researches had been conducted by different authors to study numerous variables that characterize the impinging process. Here is a short brief of researches concerned with this subject; Lytle, et. al. [1] (1994) verified the local heat transfer characteristics of air jet impingement at nozzle to plate spacing of less than one nozzle diameter, the flow structure is investigated using Laser-Doppler velocimetry. A correlation for stagnation Nusselt number was conducted based of experimental results. Zuckerman, et. al. [2] (2006) described the applications, physics of the flow and heat transfer phenomena, available empirical correlations and values they predicted, and the numerical simulation techniques and results of impinging jet devices for heat transfer. The relative strengths and drawbacks of the $k-\epsilon$, $k-\omega$, Reynolds stress model, algebraic stress models, shear stress transport, and v^2f turbulence models for impinging jet flow and heat transfer are compared. Hofmann, et. al. [3] (2007) experimentally investigated the flow structure and heat transfer from a single round jet impinging orthogonally on a flat plate. Heat transfer has been studied by means of thermography, the influence of H/D and Reynolds number Re on local heat transfer coefficient has been investigated, flow structure in a free jet has also been examined, also correlation for heat transfer coefficients have been developed. O'Donovan, et. al. [4] (2007) investigate the heat transfer distribution from a heated flat plate under impinging air jet with Reynolds number from 10000 to 30000 and $H/D = 0.5$ to 8. Results shows that at low nozzle to impingement surface spacing, $H/D < 2$, mean heat transfer distribution in the radial direction exhibits secondary peaks, also, the peak value of Nusselt number is influenced more by velocity fluctuations normal to the surface than by fluctuations parallel with the surface, this is consistent with the direction of the maximum temperature gradient. Vadiraj Katti, et. al. [5] (2008) performed an experimental investigation to study the effect of jet to plate spacing H/D and Reynolds number Re on the local heat transfer distribution to normally impinging submerged circular air jet on a smooth flat surface. Re was varied in the range of 12000-28000 and H/D of 0.5-8. A correlations for the local Nusselt number were developed from the experimental data for two ranges of $H/D \leq 3$ and For $H/D \geq 4$. Toshihiko Shakouchi, et. al. [6] (2012) conducted a detailed study on the effect of nozzle geometry on flow and heat transfer characteristics of the jet issuing from an orifice nozzle. The results show that heat transfer characteristic is governed by jet impinging velocity, flow resistance, and turbulence intensity. Locating notches on the edge of the orifice nozzle exit will

reduce the flow resistance and increase the turbulence intensity. This improve the heat transfer rates.

The above mentioned literatures give examples of the main factors that affecting the heat transfer removal in impingement process such as orifice diameter, jet velocity, H/D, turbulence level, orifice profileetc. The present work represent experimental and numerical study to characterize and correlate the heat transfer from a target plate under air jet impingement from different orifice sizes of (5,10,15,20 mm). Jet velocity is to be varied in the range 18-40 m/s and H/D in the range of 2-8. A control system is developed to carry out the impingement process with variable orifice diameter in the range of 0-45 mm. The control system is designed so that the orifice diameter is linearly changed as the target plate temperature is changed relative to a certain designed reference temperature and set by a set point (S.P) temperature.

Experimental Apparatus

Figure (1) shows a photo picture of the experimental rig and its components. The experimental apparatus consists mainly of air blower, pipe with (50 mm) diameter, a cap fitted at pipe end at which variable orifice diameters can be fixed. A straighteners (designed in accordance with British standard 1042 [7]) is fitted at impingement pipe inlet to reduce the turbulence intensity for the incoming air. The velocity range is controlled by using a bypass valve fixed near the pipe inlet. A target plate made of 30×30 cm² stainless steel (relatively low thermal conductivity of 26.1 W/m.°C) with small thickness of 0.4 mm is fitted at the test section in which the air impinges on it. A constant heat flux from heater wire of (23 Ω) resistance is used to heat the target plate. A Duralumin Alloy plate 0.6 mm in thickness (with a high thermal conductivity (177 W/m.°C) is placed between the stainless steel plate and the heater to ensure a uniform distribution to the heat within the target plate. To ensure a reliable thermal coupling and heat dissipation, a Non-Silicon heat transfer compound is used between stainless steel and Duralumin Alloy plates and heater as a heat sink. 9 cm thickness polyurethane foam layer is used to reduce the heat losses due to conduction from the lower surface of heated plate. 12 thermocouples type-K are fitted on the heated plate starting from the center to the outer edge with radial distance of 1 cm pitch. Additional two thermocouples are used to calculate the heat losses due to conduction from the lower surface of heated plate. A single thermocouple is used to measure the ambient temperature. A wooden box is used to retain the plate assembly forming the test section. Figure (2) shows test section details. A total tube 0.3 mm in diameter is used to measure air velocity distribution at orifice exit and within the wall jet region. For more details of the test rig see reference [8].

A control system with variable area orifice is designed and manufactured to obtain a variable diameters at jet exit, see figure (3). The orifice structure is made of

0.6 mm stainless steel sheets and designed to give a reliable endurance for air flow and the weight of attached parts; stepper motor, roller, cogged belt, limit switches. The orifice consists of 8 fins placed with a helical arrangement to avoid the overlapping between each other. Figure (4) shows the orifice diaphragm which is designed to flow area control requirements. An axial arm controls the orifice size with a diameter range of 0-45 mm and divided the fins into two groups each of 4 fins. Each fin has two ends, one of them is fixed with the outer cover of the orifice, and the other one is attached with the axial arm by a rivet to import the arm motion to the fin. The change from total closed position to the full opening position required 10 pulses from the stepper motor.

The control system is designed to change the orifice diameter in accordance with the difference between the desired temperature (Set Point, S.P) and the actual temperature of the target plate. Mainly two parameters are found to affect cooling rates on the heated plate, jet velocity and orifice diameter. The air jet velocities are normally limited by the noise encountered during impingement process and by blower characteristics. Usually small orifice sizes gives a limitation in blower operation due to flow choking problems, hence, as will be shown later better cooling characteristics are gained with the bigger tested orifice size. Hence the control system is designed to start with the bigger possible orifice size, then the change in diameter will continue until the plate temperature reaches the desired limit (S.P). Rate of orifice diameter change is specified by programming the microcontroller. Figure (5) shows a schematic and block diagram of the control system.

The control system consist of main three parts; temperature sensor, control board, and the variable area orifice. The thermocouple wires ends are provided with PCC-SMP connector which is compatible with (THERMO Click) add-on board. The control board include the electronic parts of the control system as clarified in figure (6). There are two operation mode for the control system; mode A is the control mode while mode B is the Set Point mode. When mode B is activated the (S.P) could be changed by pressing the red buttons to increase or decrease the value, under this mode the motor and the thermocouple doesn't works. When mode A is a activated the procedure that shown in figure (7) will be execute.

Numerical Simulation

The numerical solution is used to validate the experimental results and to check for different variables affecting cooling characteristics of air jet impingement on the target plate. The computational fluid dynamic (CFD) model is constructed based on test description and using the software package Fluent provided by ANSYS Workbench 14.5.

The governing equations used in the present investigation are continuity, momentum, energy, and turbulence scales k and ϵ all have the general form:

$$\frac{\partial}{\partial x}(\rho u \phi) + \frac{\partial}{\partial y}(\rho v \phi) + \frac{\partial}{\partial z}(\rho w \phi) = \frac{\partial}{\partial x} \left(\Gamma_{\phi} \frac{\partial \phi}{\partial x} \right) + \frac{\partial}{\partial y} \left(\Gamma_{\phi} \frac{\partial \phi}{\partial y} \right) + \frac{\partial}{\partial z} \left(\Gamma_{\phi} \frac{\partial \phi}{\partial z} \right) + S_{\phi} \quad \dots (1)$$

For more details about governing equations and discretization see reference [8].

The computational domain used for the flat plate jet impingement simulation is shown in figure (8). The grid is made up with a total of 165834 nodes and 885582 elements with high smoothing and growth rate of 1.1. The model consists of an enclosure which has the same dimensions as that of the cabinet used in the experimental study, the stainless steel plate which has the dimensions (30×30 cm²) is placed at the bottom surface of the enclosure. Heat flux boundary condition is applied to the bottom surface of the stainless steel plate, the shell conduction option is considered for the present investigation taken into account the conduction effect within the plate material. A circular tube having diameter same as that of the jet is protruding in to the top side of enclosure, this plane is set as an inlet boundary condition with specified jet velocity and temperature. The side and top planes of the enclosure considered as an pressure outlet boundary condition. The value of each boundary condition variable has been conducted from the experimental tests. Figure (9) shows the designed model and computational domain that was used in this study. The solution is initialized using the standard initialization method with 1000 iterations, the absolute criteria for the convergence checking was 1*10⁻⁵ for all residual equations (continuity, velocity, energy, k-ε).

Results and Discussions

Measurements of the experimental part of this work deals with velocity distributions, heat transfer coefficients, temperature distributions at different H/D values. Numerical work is used to validate the experimental results. Control system design is based on experimental results and used to increase the heat removal rate by increasing the orifice size within the designed limits of the injection pipe as will be mentioned later.

Velocity measurements in the exit region and beyond it shows that the jet for different orifice sizes tested is characterized by the potential, transition, and free jet regions. Smaller orifice is with shorter potential core while relatively bigger sizes are with larger one. As jet move more in the axial direction it becomes wider and takes bell shape. Higher jet velocities are with smaller width while smaller jet velocities are wider. Figure (10) shows an example of jet velocity distribution for orifice diameter D=20 mm.

Example of wall jet velocity distributions starting from stagnation point on the target plate and moving outward in radial direction for orifice diameter D=20 mm and U_j=37.4 m/s is shown in figure (11). The distribution shows high velocity in the radial direction on the wall with small layer thickness (δ) at stagnation zone. Progressly as wall jet moves outward its thickness increases with lower velocity

distribution values. Velocity distribution in the orifice exit and wall jet regions are with the same trend of experimental measurements for different authors as Hofmann [3] and Vachirakornwattana [9]. The area covered by the wall jet region after which the wall jet velocities diminishes is examined for different orifice sizes and optimum H/D values and is represented in table (1). Which shows that lower velocity at jet exit corresponds to a wider distribution in the radial direction from the jet center, i.e. a wider zone covered by the jet.

Table (1). Dimensionless presentation of jet distribution.

| Orifice diameter | Distribution range |
|------------------|--------------------|
| D=5 mm | r/R = 2.5 – 3 |
| D=10 mm | r/R = 2.4 – 2.8 |
| D=15 mm | r/R = 2 – 2.5 |
| D=20 mm | r/R = 1.8 – 2 |

A thermal image is taken to the heated target plate to examine the temperature distribution on the plate. Figure (12) shows thermal image for D=20 mm and U_j=37.4 m/s. Temperature values and distribution at plate surface is confirmed by thermocouples and thermal image readings and it is found to be in a very good agreement. Using thermocouples readings in radial direction and heat flux by convection equation (2) is used to determine local heat transfer coefficient distribution on the target plate.

$$h = \frac{q'' + \frac{kt}{r} \frac{d}{dr} \left(r \frac{dT}{dr} \right)}{T_s - T_f} \quad (W / m^2 . C^{\circ}) \quad \dots(2)$$

As seen in equation (2), the second term added to heat flux in the nominator represent the correction made due to heat conduction based on the temperature gradient in radial direction within the stainless steel plate [8].

Examining the effect of different height to orifice diameter ratio H/D shows that optimum H/D values which gives the highest h_{stag.} and h_{avg.} is H/D=6. Figure (13) shows a graphical representation of average heat transfer coefficients and its variation with jet velocity and H/D for D=20 mm. Other orifice sizes have the same trend. This is in agreement with other researcher results as Lytle [1] and others.

An example of local heat transfer coefficients distribution for different jet velocities and H/D values presented as Nusselt number distribution is shown in figure (14) for D=20 mm as an example. Other orifice diameters are tested in the same

manner and shows the same trend for various tested parameters. The following equation gives an empirical correlation found from experimental results for 64 tests on different orifices size (5,10,15 and 20 mm);

$$Nu_{stag} = 0.325 Re^{0.646} (H/D)^{-1.505} \quad \dots\dots(3)$$

Figure (15) shows the representation of the data represented by equation (3) and comparison with experimental results given by Lytle [1]. The correlation is found to fit the present experimental data with 10-15%, while its difference with Lytle data is within 10-20%.

The present experimental results represented by equation (3) agrees with previously published results as that given by Hofmann [3] and O'Donovan [4]. The results declared that heat transfer coefficients represented by Nusselt number are related to Re^m with m being in the range 0.5-0.7 depending on different operating variables and orifice or nozzle shape. The constant m is less than unity and being the index for Reynolds number in which Nusselt number and heat removal rate is directly related to jet velocity U_j and orifice diameter D . A discussion on the effect of these two variables will show that jet velocity is limited by the air blower characteristics and noise limitations at relatively high jet velocities, while orifice diameters is one of the size limitations.

Numerical simulation results approved the trend of the experimental results for different tested orifice sizes. Temperature contour and velocity distribution contour are shown in figure (16) for $D=20$ mm. A comparison between experimental and numerical results is shown in figure (17) with numerical values are being relatively higher. This can be discussed on different factors, mainly the turbulence modeling and experimental uncertainty.

According to the above discussion a control system is designed to give optimum orifice sizes in accordance with a certain set point related to the temperature difference between the target plate and the impinging air temperature. This will give a continuous change of orifice diameter and jet velocity (starting with a possible bigger orifice size) during the cooling process till the plate temperature reaches the desired limit (S.P). In the present work the orifice to plate spacing is taken as the optimum value $H/D=6$ fixed at each test carried out.

Velocity distribution shows a wider spreading of the impingement jet relative to the ordinary orifice with nearer size as shown in figure (18). This attributed to the sharp edges and corners formed by fins overlapping. Figure (19) shows a comparison of the measured heat transfer coefficients to an ordinary orifice. Relatively higher values are noticed with using the controlled orifice, this attributed to higher level of turbulence intensity due to the notches and edges described above and the wider effected zone of impingement. This behavior is confirmed by the experimental results of Shakouchi [6] where a notched orifice gives higher turbulence level. The enhancement of heat transfer is found to be in the range of 30-80% by using the controlled orifice.

The controlled orifice is tested in another way in which the orifice diameter is fixed first using certain value of the S.P. The time needed for cooling to reach S.P limit at stagnation point is recorded, then the control system is operated at the same S.P and the elapsed time is recorded as well. Figure (20) shows the cooling rate behavior for different orifice sizes tested which reveals that shorter times are required to reach the desired level of cooling with the use of control system. The figure also reveals that the use of control system is more effective starting with bigger orifice rather than small one.

CONCLUSIONS

The cooling rate and heat transfer coefficients distribution calculated from temperature distribution in air impingement from different orifice sizes of (5,10,15 and 20 mm) is found experimentally then compared that extracted from CFD Fluent 14.5 code. A controlled variable area orifice is then designed and tested at the optimum H/D value. The concluded remarks are as follows; Bigger orifice sizes and higher jet velocities give higher local and average values of heat transfer coefficients. The optimum value of H/D for the tested orifices is 6. Experimental data represented by stagnation heat transfer coefficients is given by an empirical correlation (Equation (3)). Heat transfer coefficients are found to be monotonically decreased with radial distance from plate center. Numerical simulation results show the same trend for the experimental results with a relative difference with higher values of Nusselt number for the numerical results attributed to the turbulence model used and experimental uncertainties. Testing the controlled orifice with certain set point (S.P) gives higher local heat transfer coefficient distribution attributed to the difference in the shape relative to the ordinary tested one and high rate of mixing and turbulence creation and the presence of sharp edges and notches in the designed controlled orifice. Transient testing and measuring of cooling time for the target plate at different set points with different orifice sizes show that the controlled orifice give shorter cooling time with higher rate of cooling as the orifice size is increased relative to the ordinary orifice. Shorter cooling times confirms the experimental results which shows that at optimum H/D, bigger orifice diameter and jet velocities are with higher local and average heat transfer rates.

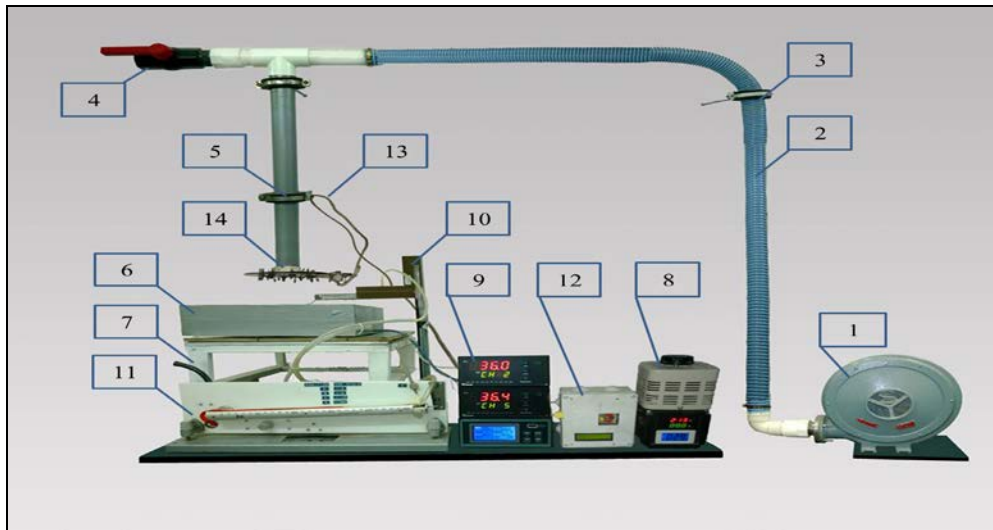


Figure (1). Experimental Rig.

1-Air Blower 2-Plastic Hose 3-Holder 4-Bypass Valve 5-P.V.C Pipe 6-Test Section 7-Adjustable Base 8-Variac + LCD Display 9-Readers 10-Traverse 11-Manometer 12-Controller Board 13-Cable 14- Controlled Orifice

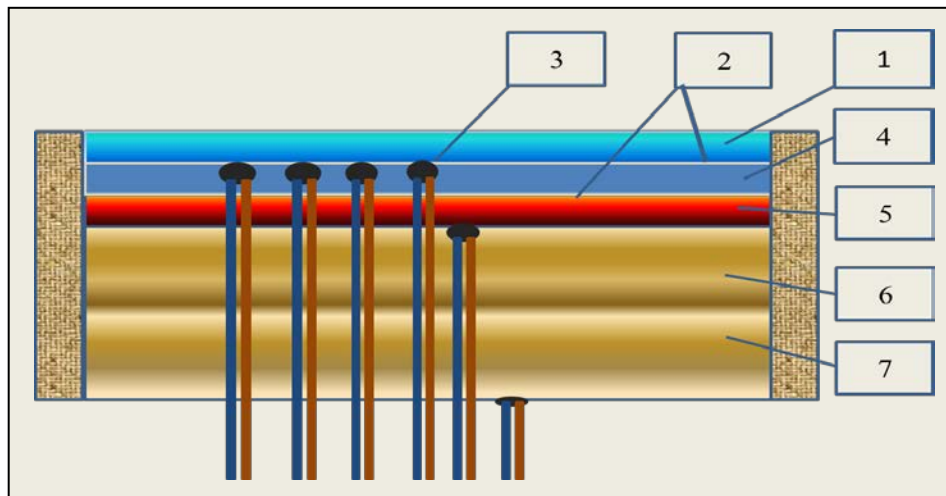


Figure (2). Test section

1-Stainless Steel Plate 2-Non-Silicon Heat Transfer Compound 3-Thermocouples Group 4-Duralumin Alloy Plate 5-Heater 6-Polyurethane Foam Layer 7-Wooden Box.

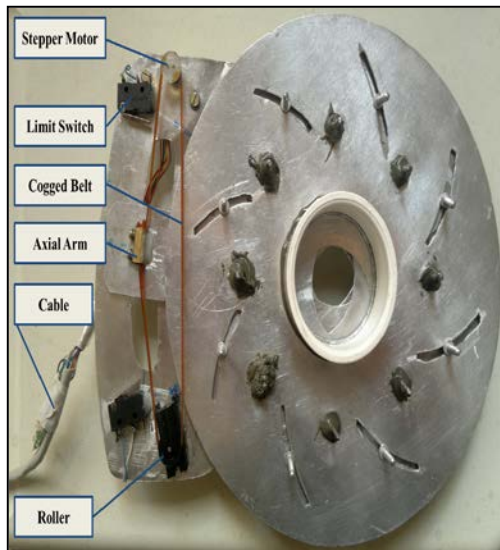


Figure (3). Variable area orifice.

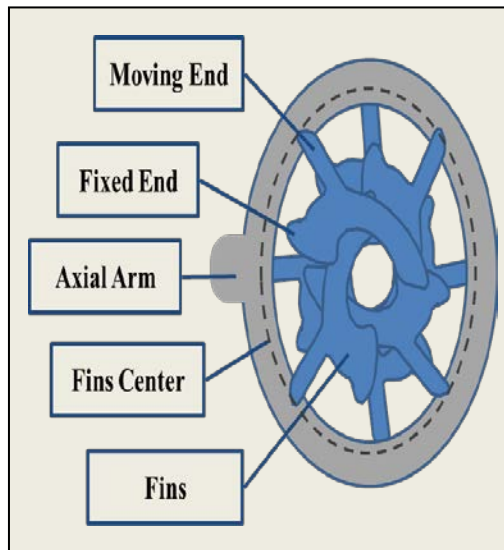


Figure (4). Orifice diaphragm.

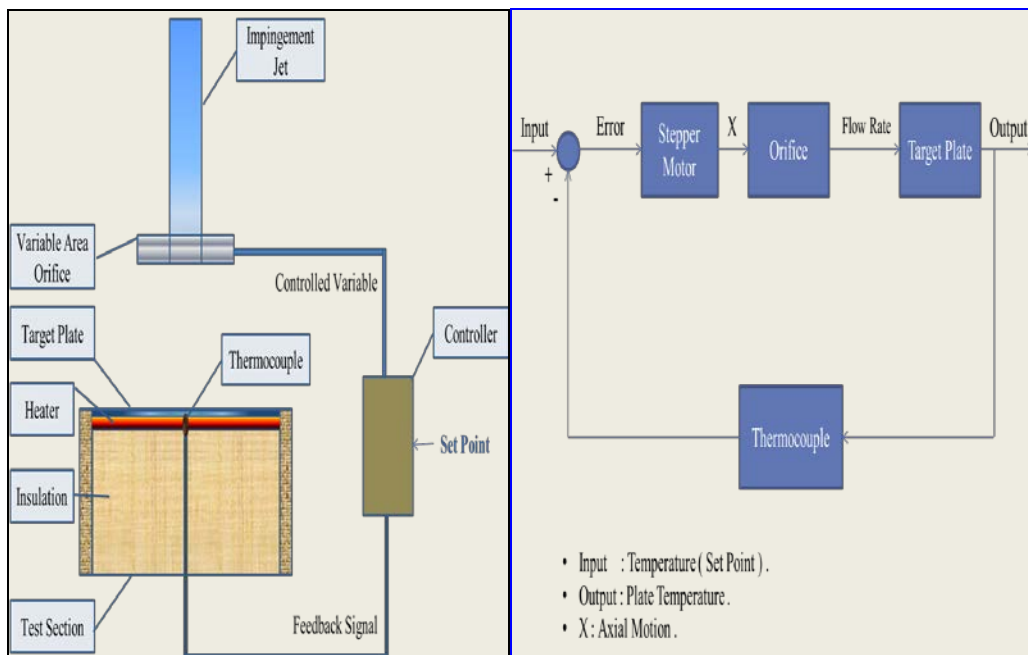


Figure (5). Schematic and demonstrated block diagram of the control system.

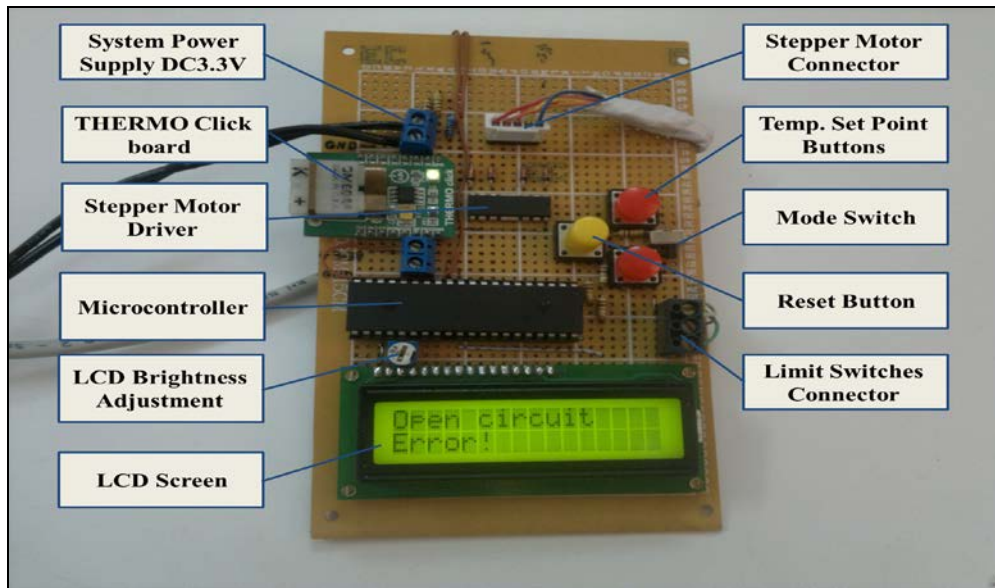


Figure (6). Control board

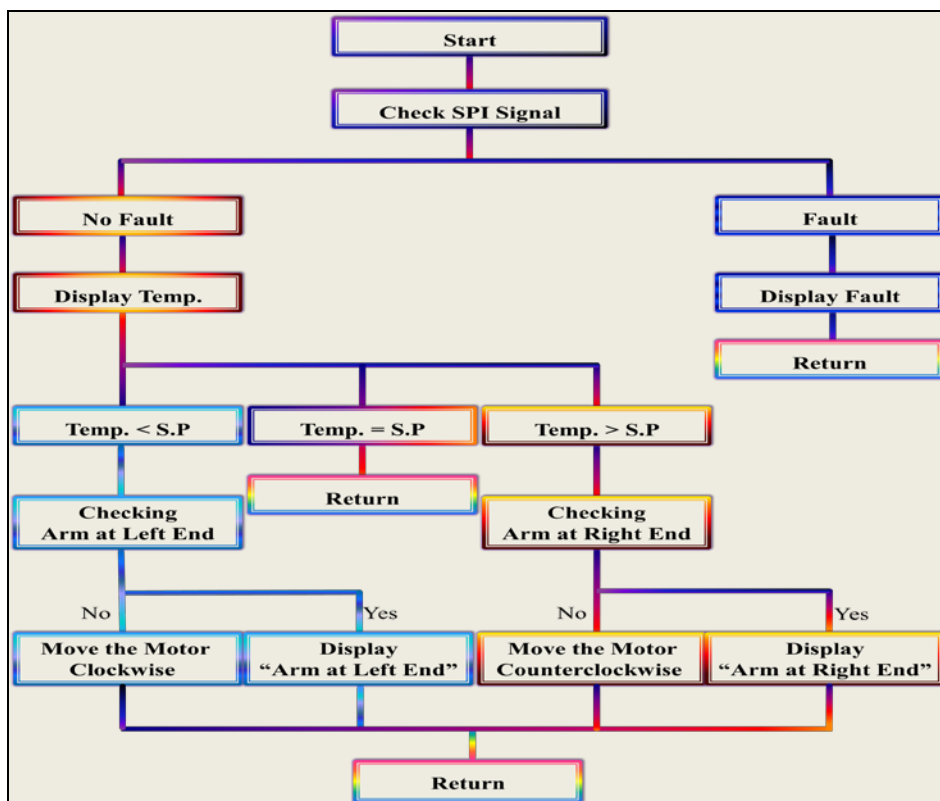


Figure (7). Procedure of the control system.

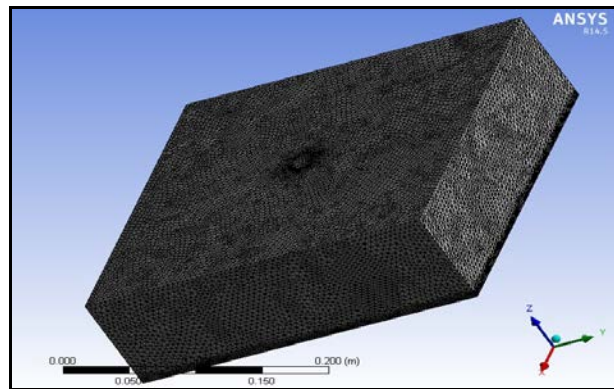


Figure (8). Computational domain with mesh.

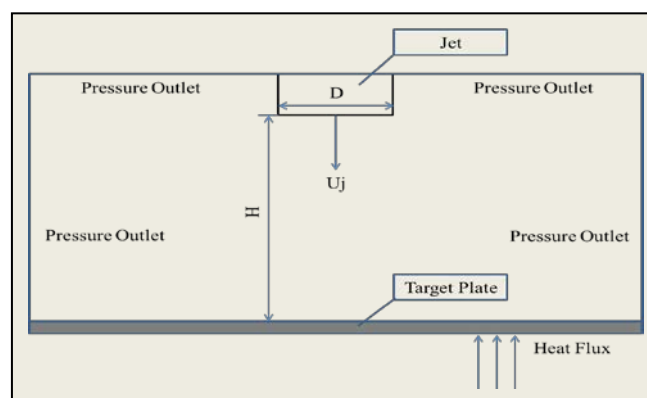


Figure (9). Designed model and computational domain.

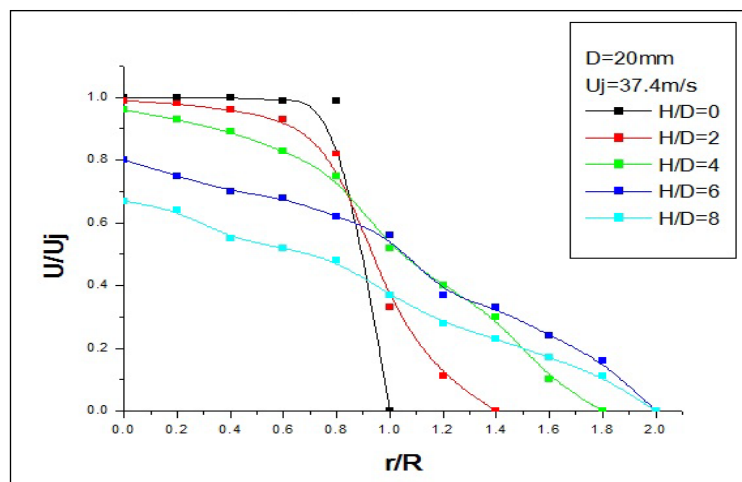


Figure (10). Velocity distribution at orifice exit. D=20mm.

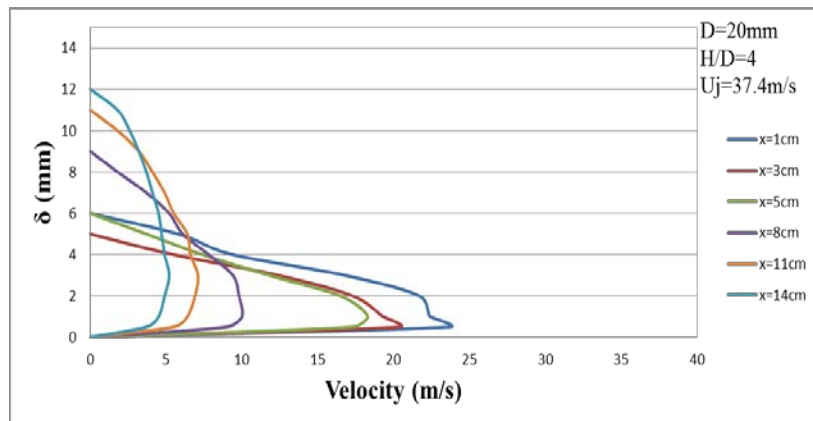


Figure (11). Boundary layer profile along the plate surface.

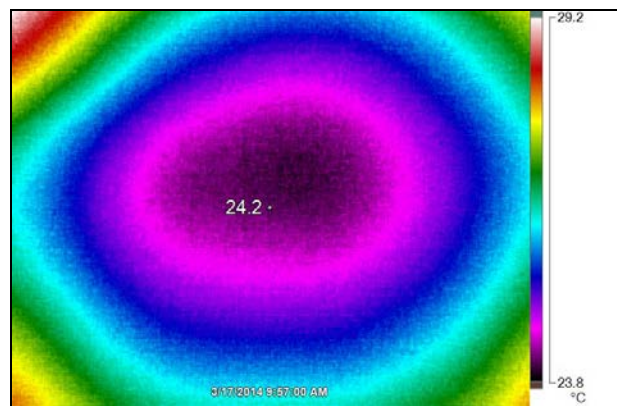


Figure (12). Thermal image.

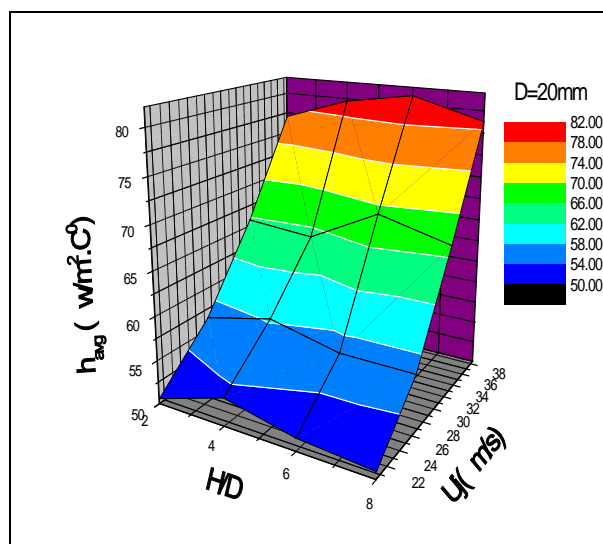


Figure (13). Graphical representation of average heat transfer coefficient, D=20mm.

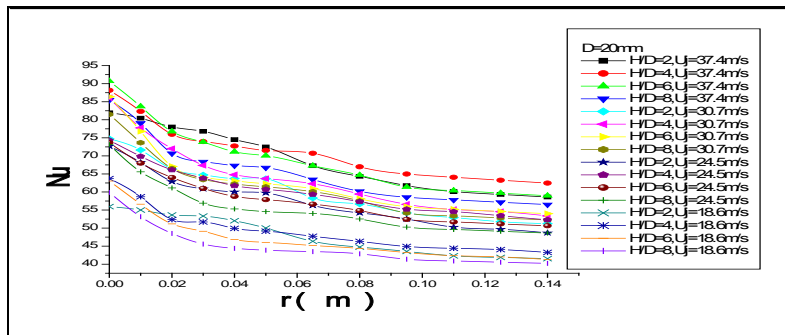


Figure (14). Local Nusselt number distribution, D=20mm.

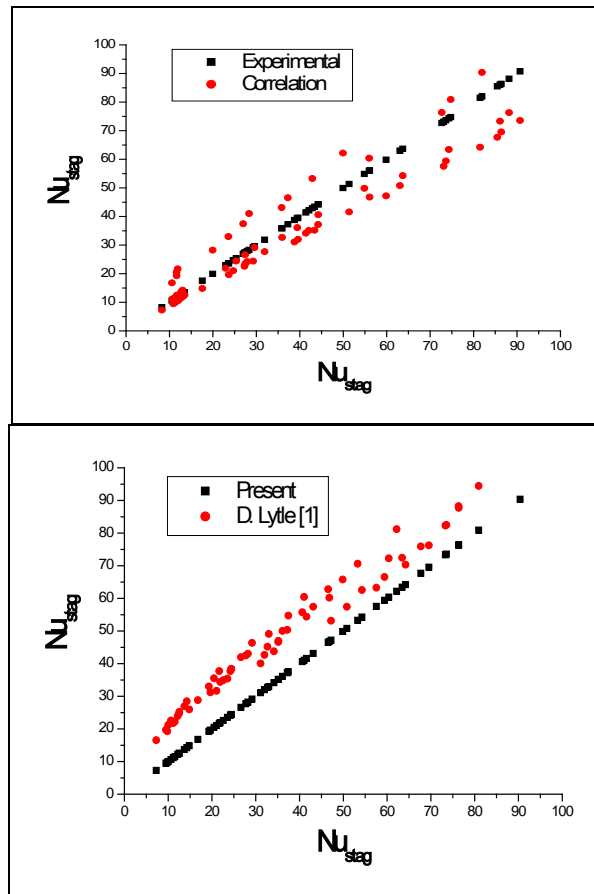


Figure (15). Data representation.

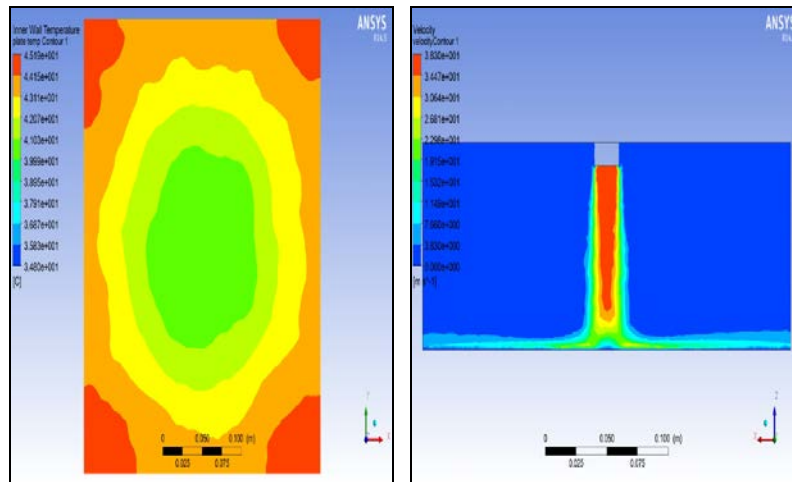


Figure (16). Temperature and velocity distribution contours, $D=20\text{mm}$.

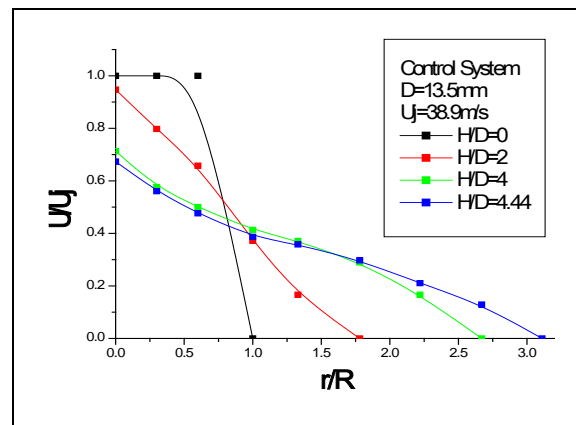


Figure (17). Local Nusselt number, $D=20\text{mm}$.

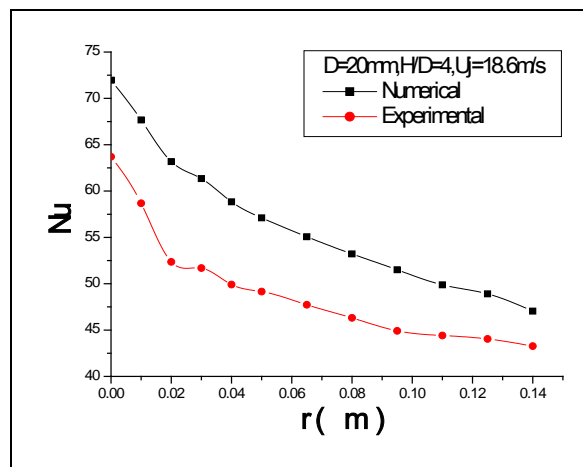


Figure (18). Velocity distribution at orifice exit, $D=13.5\text{mm}$.

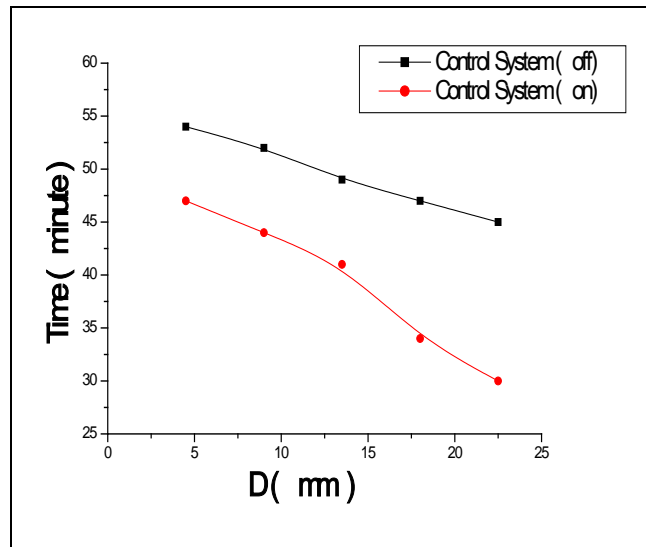


Figure (19). Local Nusselt number, H=30mm.

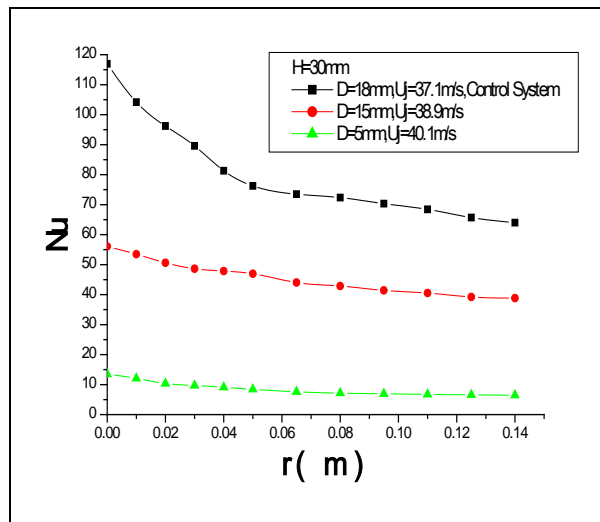


Figure (20). Comparison between two different cases (Control system off, control system on)

REFERENCES

[1].D. Lytle, B.W. Webb, 1994, "Air Jet Impingement Heat Transfer at Low Nozzle Plate Spacings", Jr. Heat Mass Transfer, Vol.37, No.12, PP.1687-1697.
 [2].N. Zuckerman, N. Lior, 2006, "Jet Impingement Heat Transfer: Physics, Correlations, and Numerical Modeling", Department of Mechanical Engineering and Applied Mechanics, The University of Pennsylvania, Philadelphia, PA, USA. Advances in Hear Transfer Jr. Vol. 39.

- [3].Herbert Martin Hofmann, Matthias Kind, Holger Martin, 2007, “Measurements on Steady State Heat Transfer and Flow Structure and New Correlations for Heat and Mass Transfer in Submerged Impinging Jets”, *International Journal of Heat and Mass Transfer*, Vol.50, pp. 3957–3965.
- [4].Tadhg S. O’Donovan, Darina B. Murray, 2007, “Jet Impingement Heat Transfer – Part I: Mean and root-mean-square heat transfer and velocity distributions”, *International Journal of Heat and Mass Transfer*, 50, pp. 3291–3301.
- [5].Vadiraj Katti, S.V. Prabhu, 2008, “Experimental Study and Theoretical Analysis of Local Heat Transfer Distribution Between Smooth Flat Surface and Impinging Air Jet From a Circular Straight Pipe Nozzle”, *International Journal of Heat and Mass Transfer*, Vol.51, pp. 4480–4495.
- [6].Toshihiko Shakouchi, Mizuki Kito, 2012, “Heat Transfer Enhancement of Impinging Jet by Notched–Orifice Nozzle”, Graduate School of Engineering, Mie University/Suzuka National College of Technology, Japan. INTECH. Chapter 15.
- [7].Fluid Flow in Closed Conduits, 1981, “British Standard Methods, Part 1”, Pressure Differential Devices, BS No.1042: Section 1.1.
- [8].Roaad K. Mohammed A., 2014, “Air Impinging Upon Target Plate Utilization Temperature Control Under Variable Flow”, A thesis submitted in partial fulfilment of the requirements for the award of Master of Science Degree in Mechanical Engineering. Al-Mustansiriya University, Baghdad-Iraq.
- [9].Jirunthanin Vachirakornwattana, 2012, “Flow structure and heat transfer of air impingement on a target plate with a single jet”, A thesis submitted in partial fulfilment of the requirements for the award of Master of Science Degree in Mechanical Engineering. Teesside University, School of Science and Engineering. UK.